

The Influence of Steric Pressure on the Structure of Homodimetallic Rhodium(I) and Iridium(I) Complexes Containing a Bis(bidentate) Phosphane Ligand

Christian Bachmann,^[a] Rene Gutmann,^[a] Georg Czermak,^[a] Alexander Dumfort,^[a] Sylvia Eller,^[a] Markus Fessler,^[a] Holger Kopacka,^[a] Karl-Hans Ongania,^[b] and Peter Brüggeller*^[a]

Keywords: X-ray diffraction / Chelates / Phosphane ligands / Iridium / Rhodium

Fifteen novel homodimetallic Rh^I and Ir^I complexes containing the bis(bidentate) phosphane ligand *cis,trans,cis*-1,2,3,4-tetrakis(diphenylphosphanyl)cyclobutane (dppcb) were prepared and characterized by NMR spectroscopy (¹H, ¹³C{¹H}, ³¹P{¹H}), mass spectrometry, IR spectroscopy, elemental analyses and melting points. Furthermore, the solid-state structures of seven of these new compounds were fully determined by single-crystal X-ray diffraction analyses to study the influence of steric pressure. The precursor complex [Rh₂(η⁴-cod)₂(dppcb)]X₂ (**1**), X⁻ = BF₄⁻, PF₆⁻, SbF₆⁻, completely characterized by its X-ray structure, smoothly reacts with mono- or bidentate ligands containing phosphorus or nitrogen donor atoms. Thus, monophosphanes and monophosphites produce compounds of the structure type [Rh₂L₄(dppcb)](SbF₆)₂ [L = PMe₂Ph, **2**; PMePh₂, **3**; P(OMe)₃, **5**; P(OPh)₃, **6**]. The X-ray structures of **3** and **6** show that PMePh₂ and P(OPh)₃ are capable of compensating steric interactions. The treatment of **1** with diphosphanes leads to the structure type [Rh₂L₂(dppcb)](SbF₆)₂ [L = bis(diphosphanyl)methane, dppm, **7**; bis(diphenylphosphanyl)amine, dppam, **8**; 1,2-bis(diphenylphosphanyl)ethane, dppe, **9**; *cis*-1,2-

bis(diphenylphosphanyl)ethene, *cis*-dppen, **10**]. The X-ray structures of **8**, **9** and **10** clearly indicate the onset of steric pressure as a consequence of mechanical coupling, which results in two different coordination moieties for homodimetallic species **9** and **10**. Under steric pressure, the quadrant effects of dppcb and dppe become comparable to Rh^I complexes. The use of mono- or bidentate ligands containing nitrogen donor atoms leads to the compounds [Rh₂(pyridine)₄(dppcb)](SbF₆)₂ (**11**), [Rh₂(2,2'-bipyridine)₂(dppcb)](SbF₆)₂ (**12**) and [Rh₂(1,10-phenanthroline)₂(dppcb)](SbF₆)₂ (**13**). The crystal structures of **1** and the novel complex [Ir₂(η⁴-cod)₂(dppcb)]X₂ (**14**), X⁻ = BF₄⁻, SbF₆⁻, are isomorphous. However, it was only possible to produce restricted examples of derivatives of **14** owing to the reluctance of **14** to release cod. Thus, monophosphanes lead to the five-coordinate species [Ir₂(η⁴-cod)₂(PMe₂Ph)₂(dppcb)](BF₄)₂ (**15**), whereas the four-coordinate compound [Ir₂(PMePh₂)₄(dppcb)](BF₄)₂ (**16**) is formed by using the sterically more demanding ligand PMePh₂ instead of PMe₂Ph.

(© Wiley-VCH Verlag GmbH & Co. KGaA, 69451 Weinheim, Germany, 2007)

Introduction

Only recently was it shown that the efficiency of catalysts containing bidentate or bis(bidentate) phosphanes is strongly determined by the flexibility of their backbones.^[1–3] This influence of the backbone can be seen in different catalytic applications like the copolymerization of carbon monoxide and ethene,^[1] the oxidative carbonylation of styrene^[2] and the Schulz–Flory oligomerization of ethene.^[3] The common feature of these different kinds of homogeneous catalysis is that square-planar complexes are thought to be responsible for the catalytic activity.^[1–3] By

contrast, it is well-known that in the case of hydroformylation the catalytically active species is a trigonal bipyramidal hydrido rhodium complex, which usually contains two phosphorus donor ligands.^[4] Because the whole catalytic cycle for the hydroformylation reaction consists of five-coordinate species,^[4] the enlargement in the coordination number relative to the above square planar catalysts certainly increases the steric pressure.^[5]

In this context, steric pressure is defined as the sum of intramolecular steric interactions keeping the coordination geometry and/or conformation of a certain complex virtually intact.^[5] This means that the onset of steric pressure enforcing intramolecular contact approaches also changes the quadrant effect^[1–3] in square planar species because the quadrant diagrams usually depend on the spatial distributions of the phenyl groups present in bidentate or bis(bidentate) phosphanes (see below, Figure 3). A certain intramolecular steric pressure only allows distinct spatial distri-

[a] Institut für Allgemeine, Anorganische und Theoretische Chemie, Universität Innsbruck, Innrain 52a, 6020 Innsbruck, Austria
E-mail: Peter.Brueggeller@uibk.ac.at

[b] Institut für Organische Chemie, Universität Innsbruck, Innrain 52a, 6020 Innsbruck, Austria

butions of these phenyl rings and hence controls the quadrant effect. Thus, steric pressure is important to determine the structure of the resultant complexes and steers their catalytic activity by the quadrant effect.^[1–3]

Therefore, in this work, the onset of steric pressure is studied in a series of X-ray structures of novel square planar homodimetallic Rh^I species containing the bis(bidentate) phosphane *cis,trans,cis*-1,2,3,4-tetrakis(diphenylphosphanyl)cyclobutane (dppcb) prepared in our laboratory.^[6] It seemed to us especially interesting to see if the rigidity of the backbone of dppcb is enough to provide the same usual quadrant effect,^[1–3] which shows one axial and one equatorial phenyl group at each phosphorus centre, even under “steric pressure”. In the case of dppcb, the onset of intramolecular steric interactions leads to excellent photochemical and photophysical properties of six-coordinate homodimetallic Ru^{II} compounds.^[7,8] However, in general, sterically congested five-coordinate complexes of Rh^I are rare and/or unstable towards the loss of the fifth ligand.^[9] In contrast, a typical situation for carbonylation catalysis is that starting square planar compounds lead to five-coordinate species.^[9,10] Therefore, a subtle choice of the steric requirements of further ligands should make it possible to observe a change in the usual conformation of the cyclobutane backbone of dppcb also in square planar Rh^I complexes, which would result in a different quadrant effect. This study should shed light on the question of whether there is sufficient flexibility in the ligand backbone of dppcb to allow easy access to all intermediates in the catalytic carbonylation cycle.^[11]

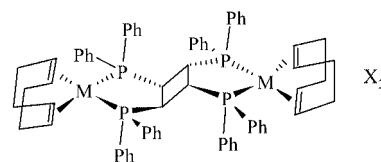
Results and Discussion

Synthesis of Complexes

[Rh₂(η⁴-cod)₂(dppcb)]X₂ (**1**), X[−] = BF₄[−], PF₆[−], SbF₆[−] (Figure 4), was prepared by a reported procedure for the in situ generation of a coordinatively unsaturated species [Rh(η⁴-cod)(acetone)₂]X from the chlorido-bridged dirhodium complex [RhCl(η⁴-cod)]₂.^[12] Treatment of [Rh(η⁴-cod)(acetone)₂]X with dppcb leads to **1** in excellent yield. The use of different anions was necessary, as only the BF₄[−] salt yielded single crystals suitable for X-ray structure analysis, PF₆[−] is the only innocent counterion under the planned catalytic hydroformylation conditions, and only the SbF₆[−] form of **1** produced further derivatives in excellent yield. The exchange of these anions was carried out by utilizing the corresponding silver salt.^[12]

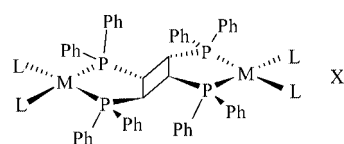
The apparent simple cod substitution from **1** makes it a suitable precursor complex.^[13] Thus, **1** smoothly reacts with the monophosphane PMe₂Ph to give [Rh₂(PMe₂Ph)₄(dppcb)](SbF₆)₂ (**2**, see Figure 1). However, in the case of the sterically more demanding monophosphane PMePh₂, not only the main product (Figure 1) [Rh₂(PMePh₂)₄(dppcb)](SbF₆)₂ (**3**) was formed, but also the known homoleptic complex^[12b] [Rh(PMePh₂)₄](SbF₆) (**4**), which was produced in a side reaction and isolated in a pure form (Figure 1). The formation of homoleptic species depending

on the steric demands of the involved ligands is typical for this kind of reaction.^[13] However, the use of the sterically congested monophosphane PPh₃ and **1** leads to a fast equilibrium between the different compounds as evidenced from the resulting ³¹P{¹H} NMR spectrum; no product could be isolated.



1: M = Rh; X = BF₄, PF₆, SbF₆

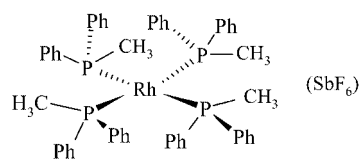
14: M = Ir; X = BF₄, SbF₆



M = Rh; X = SbF₆; **2**: L = P(CH₃)₂Ph, **3**: L = P(CH₃)Ph₂,

5: L = P(OCH₃)₃, **6**: L = P(OPh)₃

M = Ir; X = BF₄; **16**: L = P(CH₃)Ph₂



4

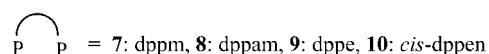
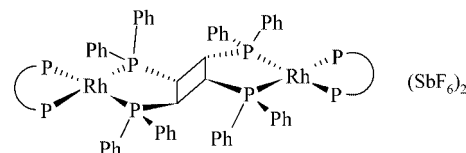


Figure 1. Structure types observed in Rh and Ir complexes.

Phosphanes can be sterically and electronically modified.^[14] Because the propensity for incremental tuning is crucially important in catalysis,^[14] we successfully extended the reaction sequence above to phosphites, diphosphanes and mono- and bidentate nitrogen ligands (see complexes **5–13** in Figures 1 and 2). Only this synthetic effort made it possible to obtain a series of X-ray structures containing increasingly sterically more-demanding ligands and to study their fine tuning of the conformation of dppcb. It was especially hoped that the onset of steric pressure could lead to different coordination units within these homodimetallic species.

In the case of Ir^I, the analogous reaction sequence leading to **1** was unsuccessful. However, as observed previously^[15] for a comparable synthesis, it was possible to perform the direct reaction of dppcb with the chlorido-bridged

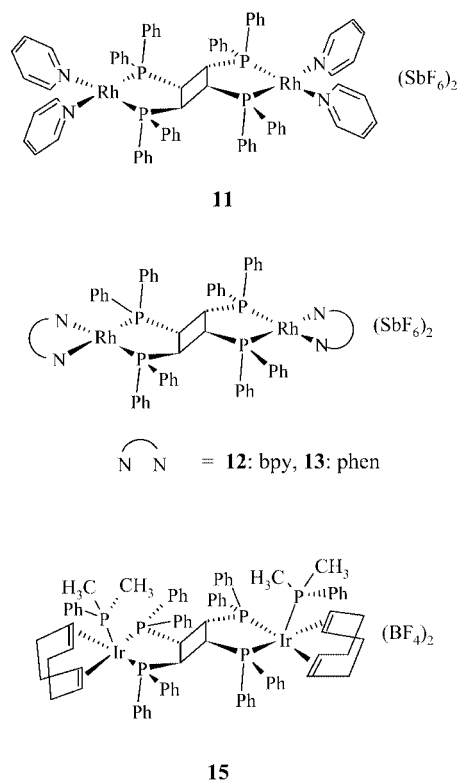


Figure 2. Structure types observed in Rh and Ir complexes.

diiridium complex $[\text{IrCl}(\eta^4\text{-cod})]_2$ and $[\text{Ir}_2\text{Cl}_2(\eta^4\text{-cod})_2(\text{dppcb})]$ resulted in excellent yield. Subsequent treatment with AgX produced $[\text{Ir}_2(\eta^4\text{-cod})_2(\text{dppcb})]\text{X}_2$ (**14**), $\text{X}^- = \text{BF}_4^-, \text{SbF}_6^-$ (see Figure 1).^[15]

Analogous to **1**, only the BF_4^- salt of **14** yielded single crystals that were suitable for X-ray structure analysis; the crystal structures of **1** and **14** are isomorphous. However, synthetic difficulties appeared when **14** was used as a precursor complex for further derivatives in its BF_4^- as well as SbF_6^- forms. Similar observations were made when other chelating ligands were treated with iridium precursor complexes and even under harsh conditions it was not possible to displace the remaining cod ligand; decomposition occurred instead.^[11] This is in agreement with the higher degree of metal-to-cod bonding and back-bonding in the iridium complexes than in the rhodium complexes and hence with the greater stability of the Ir–cod compounds.^[16] Because the ligand exchange reactions observed in Rh^I and Ir^I systems are likely to proceed by associative mechanisms,^[13] **14** smoothly reacts with the monophosphane PMe_2Ph to give the five-coordinate species $[\text{Ir}_2(\eta^4\text{-cod})_2(\text{PMe}_2\text{Ph})_2(\text{dppcb})](\text{BF}_4)_2$ (**15**, see Figure 2). Pentacoordinated structures containing cod are well-known for Ir^I,^[17] they are much more stable than the Rh^I complexes (compare analogous complexes **2** and **15** in Figures 1 and 2).

However, the greater steric pressure of PMePh_2 leads to the displacement of cod in **14** and the four-coordinate compound $[\text{Ir}_2(\text{PMePh}_2)_4(\text{dppcb})](\text{BF}_4)_2$ (**16**, Figure 1) is formed.

Interestingly, the substitutional lability of 1,5-cod versus triorganophosphane ligands does not play any role in the

clean synthesis of **1** or **14**, though this lability is consistent with predictions that are based on hard–soft acid–base theory where the soft olefin ligand is replaced preferentially by a soft triorganophosphane donor.^[18] However, as a consequence of the intrinsic problem of pentacoordination in the Ir^I case it was not possible to obtain the same series of complexes as for those of Rh^I, which reflected increasing steric pressure.

Comparison of the Quadrant Effects in Complexes of dppe and dppcb

Conformations and quadrant diagrams for $\text{M}(\text{dppe})$ and $\text{M}_2(\text{dppcb})$ complexes are shown in Figure 3.^[19] The conformation adopted by the phenyl groups in dppe complexes is noticeably different from that for the dppcb ligand. In terms of the quadrant effect, the steric crowding provided by the phenyl groups is diagonally disposed with respect to the coordination plane in the dppe derivatives. By contrast, this steric crowding is usually concentrated on one side of the coordination plane in the dppcb complexes owing to spatial distributions of the phenyl substituents on the phosphorus donors so that the two axial phenyl rings are located on the same side of the coordination plane.^[2,19] However, it is clear that the conformations shown in Figure 3 are only the borderline cases.

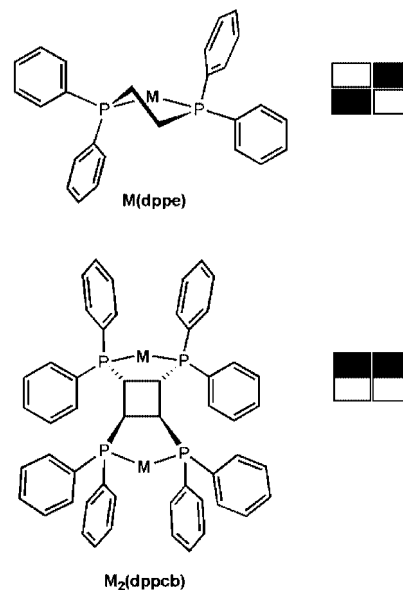


Figure 3. Quadrant effects in complexes of dppe and dppcb.

Especially for $\text{M}_2(\text{dppcb})$, a centrosymmetric structure is depicted where each coordination unit contains two axial and two equatorial phenyl groups. This conformation is typical for homodimetallic species of dppcb without steric pressure.^[1–3,6,20] The distances of the *ipso* carbon atoms of the phenyl substituents from the coordination planes clearly define axial, equatorial and diagonal dispositions (see Figure 3). Thus, the influence of the onset of steric pressure on the idealized $\text{M}_2(\text{dppcb})$ conformation in Figure 3 can be directly measured.

Isomorphous X-ray Structures of $[M_2(\eta^4\text{-cod})_2(\text{dppcb})](\text{BF}_4)_2$ [$M = \text{Rh}$ (**1**), Ir (**14**)]

It is well-known that the time-averaged preferred conformations of the five-membered metallarings in complexes of type **1** (see Figure 1) are dictated by the nature of the bidentate or bis(bidentate) phosphane ligand.^[2] The X-ray structure of **1** (see Figure 4) clearly reveals that only the phenyl groups attached to P(2) show axial and equatorial spatial distributions with respect to the coordination plane.

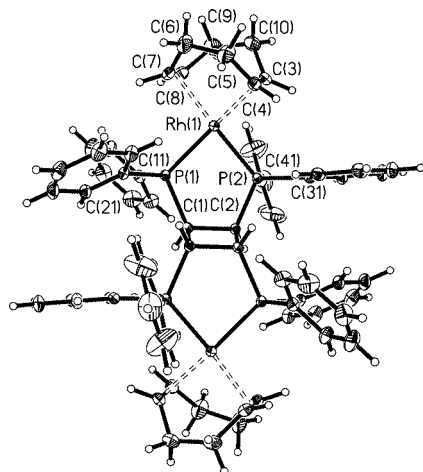


Figure 4. View of the cation of $[\text{Rh}_2(\eta^4\text{-cod})_2(\text{dppcb})](\text{BF}_4)_2$ (**1**). The atom labelling scheme is shown.

The diagonal disposition of the phenyl substituents at P(1) is characteristic of dppc.^[2,19,21] This difference is shown by the deviations of the four *ipso* carbon atoms C(11), C(21), C(31) and C(41) of $-1.177(4)$, $1.650(4)$, $0.187(5)$ and $-2.079(5)$ Å, respectively, from the coordination plane defined by the atoms Rh(1), P(1) and P(2) and the centres of gravity of the cod double bonds (see Figure 4).^[22] The largest deviations for C(21) of $1.650(4)$ Å and for C(41) of $-2.079(5)$ Å indicate that the diagonal quadrants are more hindered (see Figures 3 and 4). Obviously the steric pressure introduced by cod is already enough to change the usual quadrant effect of $M_2(\text{dppcb})$ in Figure 3. The atoms and centres of gravity (C_g) defining the coordination plane are tetrahedrally distorted, as shown by the deviations from this plane: Rh(1) $0.038(2)$ Å, P(1) $0.267(2)$ Å, P(2) $-0.289(2)$ Å, C_{g1} $0.284(3)$ Å, C_{g2} $-0.301(3)$ Å.

It was shown that short intramolecular contacts due to steric pressure in homodimetallic complexes of dppcb change their photochemical and photophysical properties.^[7,8] In the case of **1**, this steric pressure is clearly responsible for the observed unusual quadrant effect. Thus, in **1** the shortest intramolecular contact between the phenyl rings along a *trans* axis of the cyclobutane ring is C(22)⋯H(46B) of 2.988 Å. Furthermore, the hydrogen atoms attached to the double bonds of cod (see Figure 4) also show pronounced intramolecular interactions with adjacent phenyl groups: H(3A)⋯H(42A) 2.980 Å, H(4A)⋯H(36A) 2.475 Å, H(7A)⋯H(22A) 2.764 Å, H(8A)⋯H(12A) 2.558 Å. As a consequence, the C=C bonds of the cod ring are not coordinated perpendicular to the P(1)–Rh(1)–P(2) plane

and a dihedral angle of $22.5(1)^\circ$ with the C_{g1} –Rh(1)– C_{g2} plane occurs. In **1**, the distortion from an ideal square-planar coordination is larger than that in $[\text{Rh}(\eta^4\text{-cod})\{\text{CH}_2\text{P}(\text{C}_6\text{H}_4\text{-SiMe}_2\text{CH}_2\text{CH}_2\text{C}_6\text{F}_{13}\text{-}p)_2\}_2](\text{BPh}_4)$ with a corresponding dihedral angle of 13.1° ,^[21] though the steric crowding of the latter complex is considerable. A further indication of steric pressure in **1** is the significantly different Rh–C distances,^[21,23] where selected bond lengths and angles of **1** and **14** are given in Table 1.

Table 1. Selected bond lengths [Å] and angles [°] for **1** and **14**.

Compound 1		Compound 14	
Rh(1)–P(1)	2.2797(7)	Ir(1)–P(1)	2.2775(13)
Rh(1)–P(2)	2.2671(7)	Ir(1)–P(2)	2.2815(13)
Rh(1)–C(3)	2.264(3)	Ir(1)–C(3)	2.192(6)
Rh(1)–C(4)	2.227(3)	Ir(1)–C(4)	2.242(6)
Rh(1)–C(7)	2.276(3)	Ir(1)–C(7)	2.200(5)
Rh(1)–C(8)	2.234(3)	Ir(1)–C(8)	2.225(6)
C(3)–C(4)	1.368(5)	C(3)–C(4)	1.360(11)
C(7)–C(8)	1.361(6)	C(7)–C(8)	1.396(9)
P(1)–Rh(1)–P(2)	83.65(2)	P(1)–Ir(1)–P(2)	84.45(4)

However, these Rh–C distances are significantly shorter than in *cis*- $[\text{Rh}(\eta^4\text{-cod})\{\text{Me}_2\text{Si}(\mu\text{-}i\text{Bu})_2\text{PCH}_2\}_2](\text{BF}_4)$ with an average Rh–C distance of $2.305(6)$ Å.^[14] The latter long rhodium–carbon bonds were interpreted in terms of an increased steric repulsion between the bis(phosphane) and the cyclooctadiene moieties.^[14] Obviously, in **1** the steric pressure is efficiently released by a suitable distortion of the square-planar coordination together with a suitable spatial distribution of the phenyl substituents leading to an unusual quadrant effect for homodimetallic species of dppcb.

The structures of **1** and **14** fulfill the criteria of the same ligands, the same coordination number and geometry, isomorphous crystal lattices and equal experimental conditions, and, therefore, allow an exact comparison of their geometric features.^[24] The quadrant effect in **14**, given by the deviations of the four *ipso* carbon atoms C(11), C(21), C(31) and C(41) of $-1.169(5)$, $1.647(5)$, $0.217(6)$ and $-2.080(5)$ Å, respectively, from the coordination plane defined as above, is nearly identical to **1**. The same is true for the tetrahedral distortion of the coordination plane, as shown by the deviations from this plane: Ir(1) $0.032(2)$ Å, P(1) $0.272(2)$ Å, P(2) $-0.289(2)$ Å, C_{g1} $0.297(3)$ Å, C_{g2} $-0.311(3)$ Å and the resulting dihedral angle defined as above of $23.0(1)^\circ$. Also, the steric pressure of **14** is comparable to **1** (see above): C(22)⋯H(46B) 2.982 Å, H(3A)⋯H(42A) 2.908 Å, H(4A)⋯H(36A) 2.417 Å, H(7A)⋯H(22A) 2.729 Å, H(8A)⋯H(12A) 2.602 Å. However, the mean value of the significantly shorter Ir–C distances (see Table 1) of $2.196(4)$ Å in **14** is significantly shorter than the corresponding parameter of $2.231(2)$ Å in **1**. Analogously, the mean value of the significantly longer Ir–C distances of $2.234(4)$ Å is significantly shorter than the corresponding parameter of $2.270(2)$ Å in **1**.

Olefins such as cod are generally considered to be rather weakly binding ligands.^[11] However, the possibility of a pre-organization of the metal binding site leads to the formation of especially stable complexes and the olefin is not dis-

placed in the catalytically active species.^[11] It was shown above in the cases of **1** and **14** that a reorganization of dppcb, which results in the coordination of cod, produces a suitable quadrant effect and a tetrahedrally distorted coordination sphere that are responsible for the tighter binding of cod. As a consequence, the C=C bond lengths of cod are elongated in these complexes, which is normal for diene complexes of this type.^[16] The mean values of the cod double bond lengths are 1.365(4) Å in **1** and 1.378(7) Å in **14**. Thus, the bond lengthening in the iridium complex is slightly more pronounced, which is in agreement with its higher degree of metal-to-ligand bonding and back-bonding.^[16] This is in line with the significantly longer mean value of the M–centroid distances of 2.145(2) Å in **1** relative to the corresponding parameter of 2.105(4) Å in **14**. Though the M–cod *trans* influence is smaller than the M–C *trans* influence of organic groups,^[25] the significantly longer M–centroid mean value in **1** produces a significantly shorter mean value of the M–P bond lengths of 2.2734(5) Å in **1** versus 2.2795(9) Å in **14**. The use of weakly bonded olefins as leaving groups is wide-spread for rhodium catalysts.^[26] The M–C distances in **1** and **14** are located within the typical range of 2.1–2.3 Å.^[15,17,18,27] However, the significantly longer mean value of the M–centroid distances in **1** than in **14** nicely corresponds to the fact that cod is easily displaced in the case of **1**, whereas difficulties appear using **14** as a precursor complex as a result of the five-coordinate species that still contains cod.

X-ray Structures of [Rh₂(PMePh₂)₄(dppcb)](SbF₆)₂ (**3**), [Rh(PMePh₂)₄](SbF₆) (**4**) and [Rh₂{P(OPh)₃}₄(dppcb)](SbF₆)₂ (**6**)

To confirm the observation that steric pressure changes the quadrant effect in homodimetallic species of dppcb such as **1** and **14**, a series of X-ray structures showing increasing steric pressure were analyzed. Figure 5 clearly shows that in **3** the phenyl rings at P(1) are diagonally disposed with respect to the coordination plane, whereas the phenyl groups attached to P(2) show axial and equatorial spatial distributions. This means that the quadrant effect in **3** is similar to **1** and **14** (compare with Figure 4). In all cases, this influence on the quadrant effect by conformational restraints can be referred to as mechanical coupling in analogy to the concept of molecular mechanics strain energy.^[28] As in the field of molecular mechanics, mechanical coupling refers to the energy terms associated with bond stretches, bond angle bends, torsional deformations, van der Waals and electrostatic interactions.^[28]

Obviously, the steric pressure imposed by cod in **1** and **14** is comparable to two PMePh₂ moieties in **3**. Thus, the deviations of the four *ipso* carbon atoms C(11), C(21), C(31) and C(41) from the coordination plane defined by the atoms Rh(1), P(1), P(2), P(3) and P(4) are –1.175(6), 1.534(5), 0.237(5) and –2.022(6) Å, respectively (see Figure 5). These deviations are almost identical to the corresponding parameters of **1** and **14** (see above), where the

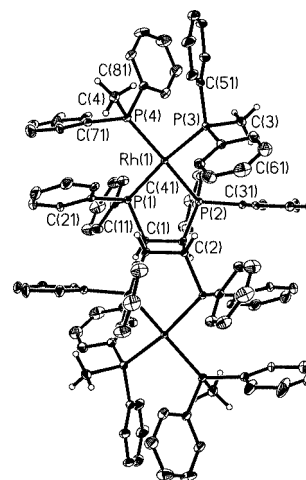


Figure 5. View of the cation of [Rh₂(PMePh₂)₄(dppcb)](SbF₆)₂ (**3**). The atom labelling scheme is shown. Hydrogen atoms attached to the phenyl rings are omitted for clarity.

largest deviations for C(21) of 1.534(5) Å and for C(41) of –2.022(6) Å again indicate that the diagonal quadrants are more hindered. Also, in **3** the coordination plane is tetrahedrally distorted, as shown by the deviations from this plane: Rh(1) 0.008(1) Å, P(1) 0.303(1) Å, P(2) –0.305(1) Å, P(3) 0.261(1) Å, P(4) –0.267(1) Å.

Although alternative ligand conformations are undoubtedly accessible in solution, the solid-state structures presented in this work exhibit trends which are consistent with steric effects exerting an important influence on reactivity.^[19] In the case of **3**, the occurrence of steric pressure leads to isolable side product **4**. The evidence of steric crowding in **3**, which is comparable to **1** and **14**, again stems from short intramolecular contact approaches. Thus, the shortest intramolecular contact between the phenyl rings along a *trans* axis of the cyclobutane ring is C(33)⋯H(22B) of 3.080 Å. The shortest intramolecular contact between the dppcb and PMePh₂ moieties is H(46A)⋯H(86A) of 2.449 Å and the shortest intramolecular contact between the PMePh₂ moieties is H(4B)⋯C(56) of 2.554 Å. As in the cases of **1** and **14**, the steric pressure in **3** is partly released by a dihedral angle of 20.7(1)° between the P(1)–Rh(1)–P(2) and P(3)–Rh(1)–P(4) planes.

The formation of homoleptic complexes such as **4** is typical for the reaction type leading to **3**.^[13] In general, the amount of tetrahedral distortion in cations [(phosphane)₄–Rh]⁺ can be rationalized as a compromise between the preferred square planar arrangement of a d⁸ transition-metal centre and the steric repulsion of the four PR₂ groups.^[13] In Figure 6 this tetrahedral distortion can be clearly seen for **4**.

The crystal structure of **4** consists of two slightly different conformations and shows dihedral angles defined as above between *cis* P–Rh–P planes of 34.5(1)° and 31.2(1)°, respectively. The Rh–P bond lengths in the two conformations of **4** are significantly shorter than the Rh–PMePh₂ distances in **3** (see Table 2). This is in line with a better release of steric pressure in **4** than in **3**, where also the elec-

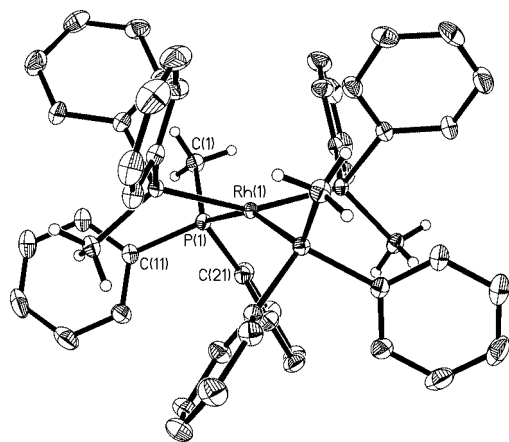


Figure 6. View of the cation of one conformation of $[\text{Rh}(\text{PMePh}_2)_4]^+$ (SbF_6^-) (**4**). The atom labelling scheme is shown. Hydrogen atoms attached to the phenyl rings are omitted for clarity.

tronic bite angle effect of dppcb could play a part.^[4] The Rh–P bond lengths of **4** are in between the average of the equatorial Rh–P bond lengths of 2.308 Å and the corresponding axial parameter of 2.337(2) Å in the distorted trigonal bipyramidal $[\text{RhH}(\text{PMePh}_2)_4]^+$.^[29] Distortions of the square planar structure like in **4** for example, also in the case of chlorotris(triphenylphosphane)rhodium(I), are well-known.^[18]

It was recognized that the quadrant effect in **1**, **3** and **14** is nearly identical and shows axial and equatorial phenyl rings attached to one phosphorus atom and diagonally disposed phenyl groups attached to the other. However, further enhancement in the steric pressure as a result of the introduction of $\text{P}(\text{OPh})_3$ leads to a change in the quadrant effect in **6**. Thus, in **6** the deviations of the four *ipso* carbon atoms C(11), C(21), C(31) and C(41) from the coordination plane defined by the atoms Rh(1), P(1), P(2), P(3) and P(4) are 0.620(5), –1.945(5), 1.480(5) and –1.394(6) Å, respectively (see Figure 7). This means that in contrast to **1**, **3** and **14**, no typical equatorial phenyl ring is present in **6** and, rather, the spatial distributions of the phenyl substituents resemble pseudoequatorial, pseudoaxial and diagonal dispositions, respectively.^[22] However, the largest deviations for C(21) of –1.945(5) Å and for C(31) of 1.480(5) Å are still in line with more hindered diagonal quadrants as in the cases **1**, **3** and **14** (see Figures 3 and 7). In **6**, the coordination plane is again tetrahedrally distorted, where the deviations from this plane are: Rh(1) 0.028(1) Å, P(1) –0.180(1) Å, P(2) 0.163(1) Å, P(3) –0.171(1) Å, P(4) 0.160(1) Å.

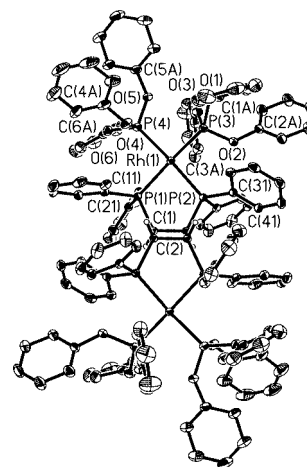


Figure 7. View of the cation of $[\text{Rh}_2\{\text{P}(\text{OPh})_3\}_4(\text{dppcb})](\text{SbF}_6)_2$ (**6**). The atom labelling scheme is shown. Hydrogen atoms attached to the phenyl rings are omitted for clarity.

For comparable (diphosphane)rhodium compounds it was found that structures determined by X-ray methods in the solid state and structures characterizing the ensembles of molecules in solution are congruent within the limits of error.^[30] This means that a change in the quadrant effect observed in the solid state is important for active catalysts derived from precatalysts such as **1**. Also, in **6** short intramolecular contact approaches are responsible for the observed conformation leading to a change in the quadrant effect compared with **1**, **3** and **14**. The shortest intramolecular contact between the phenyl rings along a *trans* axis of the cyclobutane ring is $\text{C}(34)\cdots\text{H}(26\text{B})$ of 2.910 Å. The shortest intramolecular contact between the dppcb and $\text{P}(\text{OPh})_3$ moieties is $\text{H}(16\text{A})\cdots\text{H}(6\text{BA})$ of 2.591 Å and the shortest intramolecular contact between the $\text{P}(\text{OPh})_3$ moieties is $\text{H}(1\text{BA})\cdots\text{H}(4\text{BA})$ of 2.604 Å. However, the dihedral angle of 12.4(1)° between the P(1)–Rh(1)–P(2) and P(3)–Rh(1)–P(4) planes in **6** is significantly smaller than the corresponding parameters in **1**, **3** and **14**. This means that the steric pressure in **6** is better released by a change in the quadrant effect of dppcb than by a strong tetrahedral distortion of the coordination plane.

X-ray Structures of $[\text{Rh}_2(\text{dppam})_2(\text{dppcb})](\text{SbF}_6)_2$ (**8**), $[\text{Rh}_2(\text{dppe})_2(\text{dppcb})](\text{SbF}_6)_2$ (**9**) and $[\text{Rh}_2(\text{cis-dppen})_2(\text{dppcb})](\text{SbF}_6)_2$ (**10**)

To the best of our knowledge, the X-ray structures of **8**–**10** are the first X-ray structural characterizations of rhodi-

Table 2. Selected bond lengths [Å] and angles [°] for **3**, **4** and **6**.

Compound 3		Compound 6		Compound 4	
Rh(1)–P(1)	2.2838(14)	Rh(1)–P(1)	2.3259(10)	Rh(1)–P(1)	2.3278(7)
Rh(1)–P(2)	2.3021(14)	Rh(1)–P(2)	2.3349(9)	Rh(2)–P(2)	2.3325(7)
Rh(1)–P(3)	2.3576(14)	Rh(1)–P(3)	2.2674(11)	P(1)–Rh(1)–P(1A)	92.631(7)
Rh(1)–P(4)	2.3454(13)	Rh(1)–P(4)	2.2550(10)	P(2)–Rh(2)–P(2A)	92.145(6)
P(1)–Rh(1)–P(2)	81.18(5)	P(1)–Rh(1)–P(2)	83.83(3)		
P(3)–Rh(1)–P(4)	92.67(5)	P(3)–Rh(1)–P(4)	91.30(4)		

um(I) complexes with two different chelating phosphanes. Of course, the difficulty in preparing and crystallizing these compounds stems from a further enhancement of steric pressure. As a consequence, dppcb could show the ability to form different coordination sites within homodimetallic species. This may have implications for their potential use as dimetallic catalysts, comparable to the ability of dimetallic systems with M₂P₄ units containing bis[[(diphenylphosphanyl)ethyl]phenylphosphanyl]methane to move between open and closed bridged forms.^[25] Indeed, Figures 8, 9 and 10 clearly show that the stronger steric pressure in **9** and **10**, which contain 5–5–4–5–5-membered ring systems compared with **8** that contains a 4–5–4–5–4-membered ring system, produces two different coordination sites in **9** and **10**, respectively. As all X-ray structures presented in this study show no strong intermolecular contacts or no obvious packing effect, we may assume as a first approximation that the forces on the molecule in solution are of the same order of magnitude as those in the solid.^[31] Though the crystallographic restraints are strong for structures **1**, **3**, **6**, **8** and **14** because of the presence of centres of symmetry in the middle of the cyclobutane rings, this means that centrosymmetric conformations are also available in solution for these structures. By contrast, it seems likely that **9** and **10** crystallizing in different space groups not only show noncentrosymmetric structures in the solid state, but also in solution.

Interestingly, the quadrant effect of dppcb in **8** is similar to **1**, **3** and **14**. Thus, the phenyl groups attached to one phosphorus atom show axial and equatorial spatial distributions, whereas a diagonal disposition occurs for the phenyl substituents of the other phosphorus atom (see Figure 8).

This is clearly reflected in the deviations of the four *ipso* carbon atoms C(11), C(21), C(31) and C(41) of –0.164(5), 1.912(5), 1.368(5) and –1.253(5) Å, respectively, from the coordination plane defined by the atoms Rh(1), P(1), P(2), P(3) and P(4). However, the largest deviations for C(21) of 1.912(5) Å and for C(31) of 1.368(5) Å concentrate the steric crowding now on one side of the coordination plane (see Figures 3 and 8). The atoms defining this least-squares plane are again tetrahedrally distorted, as shown by the deviations from this plane: Rh(1) 0.025(1) Å, P(1) 0.185(1) Å, P(2) –0.196(1) Å, P(3) 0.213(1) Å, P(4) –0.226(1) Å and the

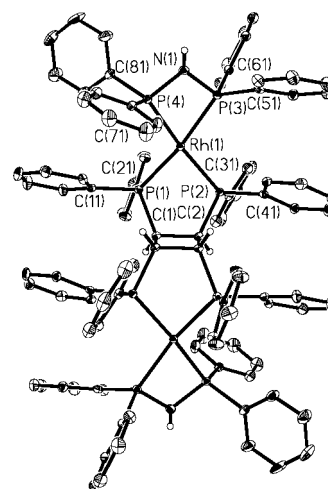


Figure 8. View of the cation of [Rh₂(dppam)₂(dppcb)](SbF₆)₂ (**8**). The atom labelling scheme is shown. Hydrogen atoms attached to the phenyl rings are omitted for clarity.

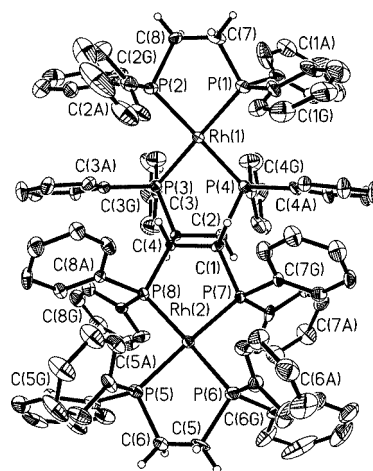


Figure 9. View of the cation of [Rh₂(dppe)₂(dppcb)](SbF₆)₂ (**9**). The atom labelling scheme is shown. Hydrogen atoms attached to the phenyl rings are omitted for clarity.

resulting dihedral angle defined as above of 16.9(1)°. Also, in this case short intramolecular contacts indicate steric crowding. The shortest contacts are 3.199 Å for H(22A)...

Table 3. Selected bond lengths [Å] and angles [°] for **8**, **9** and **10**.

Compound 8		Compound 9		Compound 10	
Rh(1)–P(1)	2.2860(10)	Rh(1)–P(1)	2.314(4)	Rh(1)–P(1)	2.305(3)
Rh(1)–P(2)	2.2909(10)	Rh(1)–P(2)	2.289(4)	Rh(1)–P(2)	2.302(3)
Rh(1)–P(3)	2.3124(10)	Rh(1)–P(3)	2.303(4)	Rh(1)–P(5)	2.287(3)
Rh(1)–P(4)	2.2937(10)	Rh(1)–P(4)	2.317(4)	Rh(1)–P(6)	2.293(3)
N(1)–H(3)	0.74(4)	Rh(2)–P(5)	2.323(4)	Rh(2)–P(3)	2.294(3)
P(1)–Rh(1)–P(2)	82.42(4)	Rh(2)–P(6)	2.314(4)	Rh(2)–P(4)	2.282(3)
P(3)–Rh(1)–P(4)	69.90(4)	Rh(2)–P(7)	2.289(4)	Rh(2)–P(7)	2.303(3)
		Rh(2)–P(8)	2.287(4)	Rh(2)–P(8)	2.310(3)
		P(1)–Rh(1)–P(2)	83.64(16)	P(1)–Rh(1)–P(2)	80.97(10)
		P(3)–Rh(1)–P(4)	81.12(13)	P(5)–Rh(1)–P(6)	83.70(13)
		P(5)–Rh(2)–P(6)	82.56(15)	P(3)–Rh(2)–P(4)	86.35(10)
		P(7)–Rh(2)–P(8)	86.63(13)	P(7)–Rh(2)–P(8)	83.48(11)

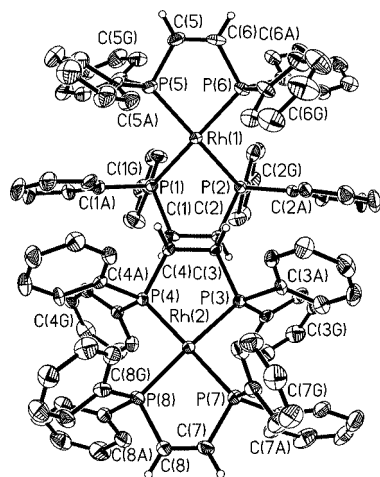


Figure 10. View of the cation of $[\text{Rh}_2(\text{cis-dppen})_2(\text{dppcb})](\text{SbF}_6)_2$ (**10**). The atom labelling scheme is shown. Hydrogen atoms attached to the phenyl rings are omitted for clarity.

H(46B) along a *trans* axis of the cyclobutane ring and 2.540 Å for H(36A)⋯H(62A) between the dppcb and dppam moieties. However, the small four-membered chelate ring angle P(3)–Rh(1)–P(4) of only 69.90(4)° (see Table 3) moves the phenyl groups of dppam away from the rhodium centre, which reduces the overall steric pressure of **8**. In contrast to **9** and **10**, this could still allow a centrosymmetric conformation for **8**. Compound **8** shows only very weak hydrogen bonds between the located N–H hydrogen atoms of dppam and the SbF_6^- counterions. This is nicely confirmed by the shorter N–H bond length of 0.74(4) Å (see Table 3) than in comparable complexes of dppam with strong hydrogen bonds (0.78–0.79 Å).^[32] Furthermore, it is also in agreement with the values of **8** for $\nu(\text{N–H})$ and $\delta(\text{N–H})$ of 3330 and 1266 cm^{-1} , respectively.^[33] It is well-known that π – π stacking of phenyl rings might play a role in tuning organometallic reactivity.^[19] Though no crystallographic restraints influence the X-ray structures of **9** and **10**, these alignments of the phenyl groups can be seen in several cases in Figures 9 and 10.

Obviously, the steric pressure is so enormous in **9** and **10** that it is necessary to minimize steric tensions through this effect. This has dramatic consequences on the conformations of **9** and **10**. The envelope-foldings, defined as the angles between the least-squares planes through the chelating phosphorus and backbone carbon atoms of dppcb and through the chelating phosphorus atoms of dppcb and the rhodium atoms, are usually orientated towards the cyclobutane rings: 20.6(1)°, **1**; 30.7(1)°, **3**; 16.5(1)°, **6**; 31.8(1)°, **8**; 20.4(1)°, **14**. The same effect is present in **9** and **10** with regard to the Rh(1) atom: 38.1(2)°, **9**; 36.8(2)°, **10**. However, the analogous envelope-foldings for the Rh(2) centres in **9** and **10** are orientated away from the cyclobutane rings: 10.0(2)°, **9**; 11.8(2)°, **10**. This inverse envelope-folding is rare for homodimetallic species of dppcb and indicative of strong steric pressure.^[7]

Indeed, the quadrant effects of dppcb become completely different for the two unequal coordination units of **9** and **10**, respectively (see Figures 9 and 10). In the cases of **9** and **10**, the phenyl rings attached to the phosphorus atoms of dppcb coordinating to the Rh(1) atoms show pseudoaxial and pseudoequatorial spatial distributions, as indicated by the deviations of the four *ipso* carbon atoms from the coordination planes defined as above: **9**, C(3A) –0.541(5) Å, C(3G) 1.653(5) Å, C(4A) –0.514(5) Å, C(4G) 1.670(5) Å; **10**, C(1A) –0.755(4) Å, C(1G) 1.619(4) Å, C(2A) –0.359(5) Å, C(2G) 1.786(5) Å. In both cases the steric crowding is concentrated on one side of the coordination plane as a result of the largest deviations for C(3G) of 1.653(5) Å and for C(4G) of 1.670(5) Å in the case of **9** and for C(1G) of 1.619(4) Å and for C(2G) of 1.786(5) Å in the case of **10** (see Figures 3, 9 and 10). In contrast, the phenyl substituents attached to the phosphorus atoms of dppcb coordinating to the Rh(2) centres unequivocally show diagonal dispositions, where the corresponding parameters are: **9**, C(7A) 1.599(5) Å, C(7G) –1.270(5) Å, C(8A) –1.373(5) Å, C(8G) 1.511(5) Å; **10**, C(3A) –1.116(5) Å, C(3G) 1.667(5) Å, C(4A) –1.446(4) Å, C(4G) 1.402(4) Å. The largest deviations corresponding to the Rh(2) centre in **9** for C(7A) of 1.599(5) Å and for C(8G) of 1.511(5) Å again concentrate the steric crowding on one side of the coordination plane (see Figures 3 and 9).

Interestingly, the analogous largest deviations in **10** for C(3G) of 1.667(5) Å and for C(4A) of –1.446(4) Å are in line with more hindered diagonal quadrants (see Figures 3 and 10). However, in **9** and **10** all deviations from the least-squares coordination planes are below 0.08 Å, as also indicated by the resulting small dihedral angles defined as above: **9**, at Rh(1) 3.3(2)°, at Rh(2) 1.8(2)°; **10**, at Rh(1) 7.4(2)°, at Rh(2) 5.0(2)°. Again, short intramolecular contacts are responsible for the observed unusual conformations. The shortest intramolecular contacts along a *trans* axis of the cyclobutane rings are 2.778 Å for C(4A)⋯H(7FA) in **9** and 2.916 Å for C(2A)⋯H(3HA) in **10**. Furthermore, the shortest intramolecular contacts are 2.310 Å for H(2HA)⋯H(3LA) between the dppcb and dppe moieties and 2.635 Å for H(6HA)⋯H(2FA) between the dppcb and *cis*-dppen moieties.

Obviously, the significantly larger five-membered chelate ring angles of dppe and *cis*-dppen in **9** and **10** relative to dppam in **8** (see Table 3) move the phenyl groups of dppe and *cis*-dppen towards the rhodium centres. This leads to overall steric pressures in **9** and **10**, which cannot be released within centrosymmetric conformations. Interestingly, though no crystallographic restraints are present, the cyclobutane rings of **9** and **10** are completely planar within statistical significance, which further confirms the similarity of the solid state to the solution structures, as discussed above. Both **9** and **10** show significantly different chelate angles of dppcb for the two unequal coordination units: **9**, 81.12(13)° and 86.63(13)°; **10**, 80.97(10)° and 86.35(10)° (see Table 3). This means that under steric pressure the chelate angles may also change, which is, beside the quadrant effect, another important feature for catalytic cycles.^[19]

Investigation of 1–3 and 5–16 in the Solution State

All compounds **1–3** and **5–16** show sharp doublets in the rhodium cases that are due to $^1J_{\text{Rh,P}}$ couplings and sharp single peaks in the iridium cases for the dppcb resonances in the $^{31}\text{P}\{^1\text{H}\}$ NMR spectra at ambient temperature. This indicates equivalent phosphorus atoms of dppcb for all complexes. Cooling the sample down to 178 K only leads to broadened signals. This behaviour is typical for dppcb conformations with planar cyclobutane rings,^[34] in contrast to folded cyclobutane ring conformations.^[6] Because planar cyclobutane rings were also observed in the X-ray structures of **1**, **3**, **6**, **8**, **9**, **10** and **14** independent of crystallographic constraints, this nicely confirms the fact that the solid-state and solution structures are identical. The structure types shown in Figures 1 and 2 are not only determined by these X-ray structures, but also their $^1J_{\text{Rh,P}}$ values of dppcb are consistent with the proposed *trans* influence series for Rh^I species.^[12a] Typically, nitrogen-containing ligands such as those in **11–13** exert a weak *trans* influence, which leads to $^1J_{\text{Rh,P}}$ parameters of 162–180 Hz. In **1** cod shows a stronger *trans* influence with $^1J_{\text{Rh,P}}$ of 154 Hz, which is characteristic of cod.^[12b] In this series, the two ligand types with the highest *trans* influence, phosphanes and phosphites,^[12a] produce $^1J_{\text{Rh,P}}$ values for dppcb of 129–137 Hz. A similar range of 121–135 Hz was observed for the corresponding $^1J_{\text{Rh,P}}$ parameters of the mono- and diphosphanes in **2**, **3** and **7–10**. The phosphites in **5** and **6** show larger $^1J_{\text{Rh,P}}$ values of 199 Hz and 234 Hz, respectively, which is also in agreement with earlier results.^[12a] The range of $^2J_{\text{P,P,trans}}$ parameters of 234–267 Hz is typical for phosphanes, where also in this case the $^2J_{\text{P,P,trans}}$ values for phosphites of 364 Hz in **5** and 380 Hz in **6** are larger.^[12a]

In **9** and **10**, the two different coordination units interchange with one another, with the asymmetric isomer being the more stable one. This leads to a coalescence of the $^{31}\text{P}\{^1\text{H}\}$ NMR signals for dppcb as well as for those of dppe and *cis*-dppen, which cannot be resolved at low temperatures. This effect is comparable to the conformational isomerisation of $[(\kappa\text{-PMes}_2\text{CH}_2\text{CH}(\text{OH})\text{CH}_2\text{-}\kappa\text{-PPh}_2)\text{-Rh}(\eta^4\text{-cod})]^+$, where δ and λ isomers interchange with one another, with the λ isomer being the more stable one.^[30] In this complex, the mesityl groups at the PMes₂ entity behave as coupled rotors, their rotation is only possible in the transformation between the δ and λ forms.^[30] In an analogous manner, the phenyl groups at the PPh₂ entities in **9** and **10** behave as coupled rotors, their rotation is only possible in the transformation between pseudoaxial and pseudoequatorial spatial distributions and diagonal dispositions of the phenyl rings of dppcb (see Figures 9 and 10). This is clearly confirmed by the observed π - π stacking interactions in **9** and **10** and could be regarded as a “mechanical molecular machine”.^[30] These conformational properties will control the stereochemical result of reactions mediated by chelate compounds of dppcb.^[35]

Summary

The series of X-ray structures presented in this work indicates that steric pressure changes the quadrant effect. It clearly proves that the rigid cyclobutane backbone of dppcb does not play any role in determining the quadrant effect, if homodimetallic Rh^I complexes of dppcb are under steric pressure. Depending on the kind and magnitude of steric pressure, both borderline cases typical for the M(dppe) and M₂(dppcb) quadrant effects in Figure 3 are observed. In consequence of which, dppcb and dppe show no differentiation between their distributions of equatorial–equatorial and equatorial–axial geometric isomers for the five-coordinate intermediates in the case of catalytic hydroformylation.^[36] However, the regioselectivity of hydroformylation is governed by a complex web of electronic and steric effects that have so far defied unravelling.^[19] Nevertheless, excellent progress was made in realizing when and how regioselectivity and enantioselectivity are controlled within a catalytic hydroformylation cycle.^[37] Our work shows that it is not enough to study the quadrant effects of precatalysts such as **1**,^[38] but it is also necessary to realize how the steric pressure varies during the catalytic cycle. Predictions solely based on X-ray structures of precatalysts such as **1** could be misleading. The occurrence of two different coordination units in **9** and **10** also seems to be of some importance for rhodium-catalysed tandem reactions.^[39]

Experimental Section

Reagents and General Procedures: The ligand dppcb was prepared as described earlier.^[6] $[\text{RhCl}(\eta^4\text{-cod})_2]$, $[\text{IrCl}(\eta^4\text{-cod})_2]$, AgX ($X^- = \text{BF}_4^-, \text{PF}_6^-, \text{SbF}_6^-$) and dry solvents of purissimum grade quality were obtained from Fluka. Mono- and diphosphanes, phosphites and nitrogen-containing ligands were purchased from Strem. A Schlenk apparatus and oxygen-free, dry Ar were used in the syntheses of all complexes. Solvents were degassed by several freeze–pump–thaw cycles prior to use. All reactions were carried out at ambient temperature.

Instrumentation: Fourier-mode ^1H , $^{13}\text{C}\{^1\text{H}\}$ and $^{31}\text{P}\{^1\text{H}\}$ NMR spectra were obtained with a Bruker DPX-300 spectrometer (internal deuterium lock) at 298 K. Positive chemical shifts are downfield from the standards: TMS for the ^1H and $^{13}\text{C}\{^1\text{H}\}$ resonances and 85% H₃PO₄ for the $^{31}\text{P}\{^1\text{H}\}$ resonances. Owing to the restricted solubility of compounds **1–16**, the $^{13}\text{C}\{^1\text{H}\}$ NMR spectra in CD₂Cl₂ are rather insensitive to structural variations, where only the $^{13}\text{C}\{^1\text{H}\}$ NMR resonances of the phenyl rings are clearly resolved in the range 128–136 ppm as multiplets.

$[\text{Rh}_2(\eta^4\text{-cod})_2(\text{dppcb})]\text{X}_2$ (1**), $X^- = \text{BF}_4^-, \text{PF}_6^-, \text{SbF}_6^-$:** $[\text{RhCl}(\eta^4\text{-cod})_2]$ (40 mg, 0.081 mmol) was dissolved in acetone (5 mL) and AgBF₄ (32 mg, 0.162 mmol) also dissolved in acetone (1 mL) was added with vigorous stirring. The reaction mixture was stirred for 3 h, and the formed AgCl was filtered off. To this solution, dppcb (64 mg, 0.081 mmol) was added with vigorous stirring. The dark orange solution was stirred for 15 min, and the solvent was then completely removed. The orange residue was washed with diethyl ether (5 mL) and dried in vacuo. Red crystals were recrystallized from CH₂Cl₂. Yield: 0.125 g (91%). M.p. 255 °C (dec.). ^1H NMR (300 MHz, CD₂Cl₂, 25 °C): δ = 6.5–8.0 (m, 40 H, Ph), 4.92 [s, 8 H,

CH (cod)], 4.30 [br. s, 4 H, *CH* (cyclobutane)], 2.41 [s, 16 H, *CH*₂ (cod)] ppm. ³¹P{¹H} NMR (121.495 MHz, CH₂Cl₂, 25 °C): δ = 72.9 (d, ¹J_{Rh,P} = 154 Hz) ppm. MS (FAB+): *m/z* (*m/z*_{calcd.}) = 1302.0 (1301.7) [M – BF₄]⁺, 607.7 (607.5) [M – BF₄]²⁺. C₆₈H₆₈B₂F₈P₄Rh₂·3.68CH₂Cl₂ (1701.07): calcd. C 50.61, H 4.47; found C 50.72, H 4.53. Single crystals suitable for X-ray structure analysis with the composition [Rh₂(η⁴-cod)₂(dppcb)](BF₄)₂·3.68CH₂Cl₂ were obtained by slow evaporation of a CH₂Cl₂ solution of the orange residue under a dry atmosphere of Ar at ambient temperature. [Rh₂(η⁴-cod)₂(dppcb)]X₂, X[–] = PF₆[–], SbF₆[–], were prepared in an analogous manner showing yields of 82 and 90%, respectively.

[Rh₂(PMe₂Ph)₄(dppcb)](SbF₆)₂ (2): [Rh₂(η⁴-cod)₂(dppcb)](SbF₆)₂ (160 mg, 0.0593 mmol) was dissolved in CH₂Cl₂ (8 mL) and PMe₂Ph (53 mg, 0.380 mmol) was added by syringe with vigorous stirring. The reaction mixture was stirred for 1 h. In the meantime, the colour of the solution changed from orange into golden brown. The solvent was completely removed, the yellow residue was washed with diethyl ether (5 mL) and dried in vacuo. A yellow powder was recrystallized from CH₂Cl₂. Yield: 0.163 g (85%). M.p. 198 °C (dec.). ¹H NMR (300 MHz, CD₂Cl₂, 25 °C): δ = 6.4–8.1 (m, 60 H, Ph), 4.31 [br. s, 4 H, *CH* (cyclobutane)], 1.08 (br. m, 24 H, *CH*₃) ppm. ³¹P{¹H} NMR (121.495 MHz, CH₂Cl₂, 25 °C): δ = 76.5 (dd, ¹J_{Rh,P} = 129 Hz, ²J_{P,P_{trans}} = 234 Hz, dppcb), –6.9 (dd, ¹J_{Rh,P} = 129 Hz, ²J_{P,P_{trans}} = 234 Hz, PMe₂Ph) ppm. MS (FAB+): *m/z* (*m/z*_{calcd.}) = 1786.9 (1786.9) [M – SbF₆]⁺, 775.5 (775.6) [M – SbF₆]²⁺. C₈₄H₈₈F₁₂P₈Rh₂Sb₂ (2022.644): calcd. C 49.88, H 4.39; found C 49.97, H 4.46.

[Rh₂(PMePh₂)₄(dppcb)](SbF₆)₂ (3): Procedure as per that of 2. Yield: 85%. M.p. 151–154 °C. ¹H NMR (300 MHz, CD₂Cl₂, 25 °C): δ = 6.3–8.2 (m, 80 H, Ph), 4.28 [br. s, 4 H, *CH* (cyclobutane)], 1.10 (br. m, 12 H, *CH*₃) ppm. ³¹P{¹H} NMR (121.495 MHz, CH₂Cl₂, 25 °C): δ = 75.1 (dd, ¹J_{Rh,P} = 137 Hz, ²J_{P,P_{trans}} = 234 Hz, dppcb), 6.6 (dd, ¹J_{Rh,P} = 129 Hz, ²J_{P,P_{trans}} = 234 Hz, PMePh₂) ppm. MS (FAB+): *m/z* (*m/z*_{calcd.}) = 2035.1 (2035.1) [M – SbF₆]⁺, 899.8 (899.7) [M – SbF₆]²⁺. C₁₀₄H₉₆F₁₂P₈Rh₂Sb₂·2CH₂Cl₂ (2440.76): calcd. C 52.16, H 4.13; found C 52.29, H 4.25. Single crystals suitable for X-ray structure analysis with the composition [Rh₂(PMePh₂)₄(dppcb)](SbF₆)₂·2CH₂Cl₂ were obtained by slow evaporation of a CH₂Cl₂ solution of 3 under an Ar atmosphere at ambient temperature.

[Rh₂{P(OMe)₃}₄(dppcb)](SbF₆)₂ (5): Procedure as per that of 2. Yield: 82%. M.p. 215 °C (dec.). ¹H NMR (300 MHz, CD₂Cl₂, 25 °C): δ = 6.5–8.0 (m, 40 H, Ph), 4.30 [br. s, 4 H, *CH* (cyclobutane)], 3.20–3.50 (m, 36 H, OCH₃) ppm. ³¹P{¹H} NMR (121.495 MHz, CH₂Cl₂, 25 °C): δ = 78.2 (dd, ¹J_{Rh,P} = 129 Hz, ²J_{P,P_{trans}} = 364 Hz, dppcb), 117.0 [dd, ¹J_{Rh,P} = 199 Hz, ²J_{P,P_{trans}} = 364 Hz, P(OMe)₃] ppm. MS (FAB+): *m/z* (*m/z*_{calcd.}) = 1730.8 (1730.7) [M – SbF₆]⁺, 747.4 (747.5) [M – SbF₆]²⁺. C₆₄H₈₀F₁₂O₁₂P₈Rh₂Sb₂ (1966.43): calcd. C 39.09, H 4.10, O 9.76; found C 39.15, H 4.20, O 9.53.

[Rh₂{P(OPh)₃}₄(dppcb)](SbF₆)₂ (6): Procedure as per that of 2. Yield: 82%. M.p. 95–98 °C. ¹H NMR (300 MHz, CD₂Cl₂, 25 °C): δ = 6.1–8.5 (m, 100 H, Ph), 4.33 [br. s, 4 H, *CH* (cyclobutane)] ppm. ³¹P{¹H} NMR (121.495 MHz, CH₂Cl₂, 25 °C): δ = 76.1 (dd, ¹J_{Rh,P} = 129 Hz, ²J_{P,P_{trans}} = 380 Hz, dppcb), 112.0 [dd, ¹J_{Rh,P} = 234 Hz, ²J_{P,P_{trans}} = 380 Hz, P(OPh)₃] ppm. MS (FAB+): *m/z* (*m/z*_{calcd.}) = 2475.2 (2475.4) [M – SbF₆]⁺. C₁₂₄H₁₀₄F₁₂O₁₂P₈Rh₂Sb₂·4.26CH₂Cl₂ (3072.97): calcd. C 50.13, H 3.69, O 6.25; found C 50.25, H 3.85, O 6.10. Single crystals suitable for X-ray structure analysis with the composition [Rh₂{P(OPh)₃}₄(dppcb)](SbF₆)₂·4.26CH₂Cl₂ were obtained by slow evaporation of

a CH₂Cl₂ solution of 6 under an Ar atmosphere at ambient temperature.

[Rh₂(dppm)₂(dppcb)](SbF₆)₂ (7): [Rh₂(η⁴-cod)₂(dppcb)](SbF₆)₂ (100 mg, 0.0593 mmol) was dissolved in CH₂Cl₂ (10 mL) and dppm (46 mg, 0.119 mmol) was added in solid form with vigorous stirring. The reaction mixture was stirred for 1 h and a clear orange solution was obtained. The solvent was completely removed, the yellow residue was washed with diethyl ether (5 mL) and dried in vacuo. A yellow powder was recrystallized from CH₂Cl₂. Yield: 0.106 g (80%). M.p. 250–253 °C. ¹H NMR (300 MHz, CD₂Cl₂, 25 °C): δ = 6.5–8.0 (m, 80 H, Ph), 4.30 [br. s, 4 H, *CH* (cyclobutane)], 2.22 (br. m, 4 H, *CH*₂P) ppm. ³¹P{¹H} NMR (121.495 MHz, CH₂Cl₂, 25 °C): δ = 79.7 (dd, ¹J_{Rh,P} = 137 Hz, ²J_{P,P_{trans}} = 259 Hz, dppcb), –18.5 (dd, ¹J_{Rh,P} = 121 Hz, ²J_{P,P_{trans}} = 259 Hz, dppm) ppm. MS (FAB+): *m/z* (*m/z*_{calcd.}) = 2238.1 (2237.8) [M – H]⁺, 2003.4 (2003.1) [M – SbF₆]⁺. C₁₀₂H₈₈F₁₂P₈Rh₂Sb₂ (2238.84): calcd. C 54.72, H 3.96; found C 54.83, H 4.03.

[Rh₂(dppam)₂(dppcb)](SbF₆)₂ (8): Procedure as per that of 7. Yield: 87%. M.p. 275–278 °C. ¹H NMR (300 MHz, CD₂Cl₂, 25 °C): δ = 6.0–8.3 (m, 80 H, Ph), 4.29 [br. s, 4 H, *CH* (cyclobutane)] ppm. ³¹P{¹H} NMR (121.495 MHz, CH₂Cl₂, 25 °C): δ = 78.5 (dd, ¹J_{Rh,P} = 137 Hz, ²J_{P,P_{trans}} = 267 Hz, dppcb), 45.9 (dd, ¹J_{Rh,P} = 121 Hz, ²J_{P,P_{trans}} = 267 Hz, dppam) ppm. IR (KBr): $\tilde{\nu}$ = 3330 (m) (N–H), 1266 (m) (N–H) cm^{–1}. MS (FAB+): *m/z* (*m/z*_{calcd.}) = 2240.2 (2239.9) [M – H]⁺, 2005.1 (2005.1) [M – SbF₆]⁺. C₁₀₀H₈₆F₁₂N₂P₈Rh₂Sb₂ (2240.81): calcd. C 53.60, H 3.87, N 1.25; found C 53.73, H 3.93, N 1.15. Single crystals suitable for X-ray structure analysis with the composition [Rh₂(dppam)₂(dppcb)](SbF₆)₂ were obtained by slow evaporation of a CH₂Cl₂ solution of 8 under an Ar atmosphere at 277 K.

[Rh₂(dppe)₂(dppcb)](SbF₆)₂ (9): Procedure as per that of 7. Yield: 83%. M.p. 140 °C (dec.). ¹H NMR (300 MHz, CD₂Cl₂, 25 °C): δ = 6.5–8.1 (m, 80 H, Ph), 4.31 [br. s, 4 H, *CH* (cyclobutane)], 2.25 (br. m, 8 H, *CH*₂P) ppm. ³¹P{¹H} NMR (121.495 MHz, CH₂Cl₂, 25 °C): δ = 81.7 (dd, ¹J_{Rh,P} = 137 Hz, ²J_{P,P_{trans}} = 241 Hz, dppcb), 54.3 (dd, ¹J_{Rh,P} = 131 Hz, ²J_{P,P_{trans}} = 241 Hz, dppe) ppm. MS (FAB+): *m/z* (*m/z*_{calcd.}) = 2267.2 (2266.9) [M]⁺, 2031.5 (2031.2) [M – SbF₆]⁺. C₁₀₄H₉₂F₁₂P₈Rh₂Sb₂·3.85CH₂Cl₂ (2593.845): calcd. C 49.94, H 3.87; found C 49.99, H 3.95. Single crystals suitable for X-ray structure analysis with the composition [Rh₂(dppe)₂(dppcb)](SbF₆)₂·3.85CH₂Cl₂ were obtained by slow evaporation of a CH₂Cl₂ solution of 9 under an Ar atmosphere at ambient temperature.

[Rh₂(*cis*-dppen)₂(dppcb)](SbF₆)₂ (10): Procedure as per that of 7. Yield: 78%. M.p. 205–207 °C. ¹H NMR (300 MHz, CD₂Cl₂, 25 °C): δ = 6.5–8.1 (m, 80 H, Ph), 6.30 (br. m, 4 H, *PCHCP*), 4.32 [br. s, 4 H, *CH* (cyclobutane)] ppm. ³¹P{¹H} NMR (121.495 MHz, CH₂Cl₂, 25 °C): δ = 76.8 (dd, ¹J_{Rh,P} = 129 Hz, ²J_{P,P_{trans}} = 259 Hz, dppcb), 66.2 (dd, ¹J_{Rh,P} = 135 Hz, ²J_{P,P_{trans}} = 259 Hz, *cis*-dppen) ppm. MS (FAB+): *m/z* (*m/z*_{calcd.}) = 2262.0 (2261.8) [M – H]⁺, 2027.5 (2027.1) [M – SbF₆]⁺. C₁₀₄H₈₈F₁₂P₈Rh₂Sb₂·5.16CH₂Cl₂ (2701.066): calcd. C 48.54, H 3.67; found C 48.64, H 3.73. Single crystals suitable for X-ray structure analysis with the composition [Rh₂(*cis*-dppen)₂(dppcb)](SbF₆)₂·5.16CH₂Cl₂ were obtained by slow evaporation of a CH₂Cl₂ solution of 10 under an Ar atmosphere at ambient temperature.

[Rh₂(pyridine)₄(dppcb)](SbF₆)₂ (11): [Rh₂(η⁴-cod)₂(dppcb)](SbF₆)₂ (100 mg, 0.0593 mmol) was dissolved in CH₂Cl₂ (7.5 mL) and pyridine (19 mg, 0.237 mmol) was added by syringe with vigorous stirring. The reaction mixture was stirred for 10 min and a clear, yellow solution was obtained. The solvent was then completely removed, and the yellow residue was washed with diethyl ether (5 mL) and

dried in vacuo. A yellow powder was recrystallized from CH₂Cl₂. Yield: 0.083 g (78%). M.p. 240–243 °C. ¹H NMR (300 MHz, CD₂Cl₂, 25 °C): δ = 8.2–9.4 (m, 20 H, pyridine), 6.6–8.1 (m, 40 H, Ph), 4.30 [br. s, 4 H, CH (cyclobutane)] ppm. ³¹P{¹H} NMR (121.495 MHz, CH₂Cl₂, 25 °C): δ = 91.3 (d, ¹J_{Rh,P} = 178 Hz) ppm. MS (FAB+): *m/z* (*m/z*_{calcd.}) = 656.2 (656.5) [M – H – SbF₆]²⁺. C₇₂H₆₄F₁₂N₄P₄Rh₂Sb₂ (1786.538): calcd. C 48.41, H 3.61, N 3.14; found C 48.53, H 3.73, N 3.07.

[Rh₂(2,2'-bipyridine)₂(dppcb)](SbF₆)₂ (12): Procedure as per that of **11** with a reaction time of 2 h. The dark red powder was recrystallized from CH₂Cl₂. Yield: 77%. M.p. 270 °C (dec.). ¹H NMR (300 MHz, CD₂Cl₂, 25 °C): δ = 8.1–9.3 (m, 16 H, bipyridine), 6.5–8.2 (m, 40 H, Ph), 4.35 [br. s, 4 H, CH (cyclobutane)] ppm. ³¹P{¹H} NMR (121.495 MHz, CH₂Cl₂, 25 °C): δ = 95.4 (d, ¹J_{Rh,P} = 162 Hz) ppm. MS (FAB+): *m/z* (*m/z*_{calcd.}) = 1547.1 (1546.8) [M – SbF₆]⁺, 1391.0 (1390.6) [M – bipyridine – SbF₆]⁺, 655.2 (655.5) [M – SbF₆]²⁺. C₇₂H₆₀F₁₂N₄P₄Rh₂Sb₂ (1782.506): calcd. C 48.52, H 3.39, N 3.14; found C 48.61, H 3.47, N 3.05.

[Rh₂(1,10-phenanthroline)₂(dppcb)](SbF₆)₂ (13): Procedure as per that of **11** with a reaction time of 40 min. The dark red powder was recrystallized from CH₂Cl₂. Yield: 81%. M.p. 260 °C (dec.). ¹H NMR (300 MHz, CD₂Cl₂, 25 °C): δ = 8.3–9.5 (m, 16 H, phenanthroline), 6.4–8.3 (m, 40 H, Ph), 4.45 [br. s, 4 H, CH (cyclobutane)] ppm. ³¹P{¹H} NMR (121.495 MHz, CH₂Cl₂, 25 °C): δ = 95.9 (d, ¹J_{Rh,P} = 180 Hz) ppm. MS (FAB+): *m/z* (*m/z*_{calcd.}) = 1594.0 (1593.8) [M – H – SbF₆]⁺, 678.9 (679.0) [M – H – 2SbF₆]²⁺. C₇₆H₆₀F₁₂N₄P₄Rh₂Sb₂ (1830.55): calcd. C 49.87, H 3.30, N 3.06; found C 49.95, H 3.41, N 3.01.

[Ir₂(η⁴-cod)₂(dppcb)]X₂ (14), X⁻ = BF₄⁻, SbF₆⁻: [IrCl(η⁴-cod)]₂ (100 mg, 0.149 mmol) was dissolved in toluene (7 mL) and dppcb (118 mg, 0.149 mmol) was added with vigorous stirring. The reaction mixture was stirred for 6 h, and the formed yellowish precipitate was filtered off. The precipitate was washed with toluene (10 mL) and dried in vacuo. The obtained yellowish powder was suspended in CH₂Cl₂/DMF (5:2, 20 mL). To this suspension was slowly added AgBF₄ (58 mg, 0.298 mmol) dissolved in CH₂Cl₂/DMF (5:2, 5 mL). Immediately an intense red solution formed. This solution was stirred for several minutes, the solvent was completely removed and the residue dried in vacuo. The residue was then suspended in CH₂Cl₂ (20 mL) and the suspension was stirred for 45 min. The formed AgCl was filtered off, the solvent of the

resulting dark red solution was completely removed and the red–brown residue was dried in vacuo. Red–brown crystals were recrystallized from CH₂Cl₂. Yield: 0.210 g (75%). M.p. 225 °C (dec.). ¹H NMR (300 MHz, CD₂Cl₂, 25 °C): δ = 6.4–8.1 (m, 40 H, Ph), 4.90 [s, 8 H, CH (cod)], 4.25 [br. s, 4 H, CH (cyclobutane)], 2.43 [s, 16 H, CH₂ (cod)] ppm. ³¹P{¹H} NMR (121.495 MHz, CH₂Cl₂, 25 °C): δ = 63.5 (s) ppm. MS (FAB+): *m/z* (*m/z*_{calcd.}) = 1480.3 (1480.3) [M – BF₄]⁺. C₆₈H₆₈B₂F₈Ir₂P₄·3.68CH₂Cl₂ (1879.69): calcd. C 45.80, H 4.04; found C 45.95, H 4.10. Single crystals suitable for X-ray structure analysis with the composition [Ir₂(η⁴-cod)₂(dppcb)](BF₄)₂·3.68CH₂Cl₂ were obtained by slow evaporation of a CH₂Cl₂ solution of the red–brown residue under a dry Ar atmosphere at ambient temperature. [Ir₂(η⁴-cod)₂(dppcb)](SbF₆)₂ was prepared in an analogous manner with a yield of 67%.

[Ir₂(η⁴-cod)₂(PMe₂Ph)₂(dppcb)](BF₄)₂ (15): Procedure as per that of **2** with 2 equiv. of the monophosphane. Yield: 67%. M.p. 168–170 °C. ¹H NMR (300 MHz, CD₂Cl₂, 25 °C): δ = 6.4–8.1 (m, 50 H, Ph), 4.80 [s, 8 H, CH (cod)], 4.26 [br. s, 4 H, CH (cyclobutane)], 2.35 [s, 16 H, CH₂ (cod)], 0.95 (br. s, 12 H, CH₃) ppm. ³¹P{¹H} NMR (121.495 MHz, CH₂Cl₂, 25 °C): δ = 36.3 (s, dppcb), –52.4 (s, PMe₂Ph) ppm. MS (FAB+): *m/z* (*m/z*_{calcd.}) = 1843.1 (1843.4) [M]⁺, 1479.4 (1479.3) [M – H – BF₄ – 2PMe₂Ph]⁺. C₈₄H₉₀B₂F₈Ir₂P₆ (1843.44): calcd. C 54.73, H 4.92; found C 54.85, H 4.98.

[Ir₂(PMePh₂)₄(dppcb)](BF₄)₂ (16): Procedure as per that of **2**. Yield: 68%. M.p. 145–147 °C. ¹H NMR (300 MHz, CD₂Cl₂, 25 °C): δ = 6.3–8.2 (m, 80 H, Ph), 4.29 [br. s, 4 H, CH (cyclobutane)], 1.05 (br. s, 12 H, CH₃) ppm. ³¹P{¹H} NMR (121.495 MHz, CH₂Cl₂, 25 °C): δ = 63.0 (d, ²J_{P,P_{trans}} = 255 Hz, dppcb), –3.1 (d, ²J_{P,P_{trans}} = 255 Hz, PMePh₂) ppm. MS (FAB+): *m/z* (*m/z*_{calcd.}) = 2065.6 (2065.9) [M + H – BF₄]⁺, 1865.4 (1865.7) [M + H – BF₄ – PMePh₂]⁺. C₁₀₄H₉₆B₂F₈Ir₂P₈ (2151.74): calcd. C 58.05, H 4.50; found C 58.19, H 4.61.

X-ray Crystallography: Details of the crystals and data collections are summarized in Tables 4 and 5. In the cases of **4** and **8**, the data collections were performed with a Nonius Kappa CCD diffractometer with the use of combined φ–ω scans. Cell refinement, data reduction and the empirical absorption correction were done by Denzo and Scalepack programs.^[40] In the cases of **1**, **3**, **6**, **9**, **10** and **14**, all data were collected with a Siemens P4 diffractometer by using ω scans. Cell refinement and data reduction were done by the software of the Siemens P4 diffractometer,^[41] and the empirical

Table 4. Crystallographic data for **1**, **14**, **3** and **4**.

Compound	1	14	3	4
Empirical formula	C ₆₈ H ₆₈ B ₂ F ₈ P ₄ Rh ₂ ·3.68CH ₂ Cl ₂	C ₆₈ H ₆₈ B ₂ F ₈ Ir ₂ P ₄ ·3.68CH ₂ Cl ₂	C ₁₀₄ H ₉₆ F ₁₂ P ₈ Rh ₂ Sb ₂ ·2CH ₂ Cl ₂	C ₅₂ H ₅₂ F ₆ P ₄ RhSb
Formula mass	1701.07	1879.69	2436.73	1139.49
Crystal system	triclinic	triclinic	triclinic	tetragonal
Space group	P $\bar{1}$	P $\bar{1}$	P $\bar{1}$	I4 ₁ /a
<i>a</i> [Å]	13.068(2)	13.054(4)	12.590(4)	16.0493(4)
<i>b</i> [Å]	13.442(2)	13.422(3)	14.504(3)	
<i>c</i> [Å]	13.686(2)	13.713(4)	16.947(2)	38.0415(6)
<i>α</i> [°]	108.23(1)	108.13(1)	69.94(1)	
<i>β</i> [°]	96.30(1)	96.66(1)	71.86(1)	
<i>γ</i> [°]	118.95(1)	118.80(1)	68.72(1)	
<i>V</i> [Å ³]	1896.9(6)	1896.2(10)	2646.2(11)	9798.7(4)
<i>Z</i>	1	1	1	8
<i>T</i> [K]	298(2)	298(2)	298(2)	298(2)
Measured reflections	9056	8364	10399	5621
Independent reflections	7978	7357	7566	5378
Final <i>R</i> ₁ , <i>wR</i> ₂ [<i>I</i> > 3σ(<i>I</i>)]	0.0392	0.0367	0.0436	0.0344
14 , 3 ; <i>I</i> > 2σ(<i>I</i>)	0.1037	0.0931	0.1013	0.0747

Table 5. Crystallographic data for **6**, **8**, **9** and **10**.

Compound	6	8	9	10
Empirical formula	C ₁₂₄ H ₁₀₄ F ₁₂ O ₁₂ P ₈ Rh ₂ Sb ₂ · 4.26CH ₂ Cl ₂	C ₁₀₀ H ₈₆ F ₁₂ N ₂ P ₈ Rh ₂ Sb ₂	C ₁₀₄ H ₉₂ F ₁₂ P ₈ Rh ₂ Sb ₂ · 3.85CH ₂ Cl ₂	C ₁₀₄ H ₈₈ F ₁₂ P ₈ Rh ₂ Sb ₂ · 5.16CH ₂ Cl ₂
Formula mass	3063.67	2240.81	2593.845	2691.41
Crystal system	triclinic	triclinic	monoclinic	monoclinic
Space group	<i>P</i> $\bar{1}$	<i>P</i> $\bar{1}$	<i>P</i> ₂ ₁	<i>P</i> ₂ ₁ / <i>n</i>
<i>a</i> [Å]	13.496(3)	13.1051(3)	13.9880(10)	17.148(3)
<i>b</i> [Å]	16.922(2)	14.1135(3)	30.376(4)	31.557(5)
<i>c</i> [Å]	18.541(2)	14.9161(3)	14.342(3)	22.126(4)
α [°]	64.06(1)	73.281(1)		
β [°]	85.44(1)	68.345(1)	107.80(1)	92.16(1)
γ [°]	69.93(1)	66.887(1)		
<i>V</i> [Å ³]	3564.0(11)	2325.18(9)	5802.2(15)	11965(4)
<i>Z</i>	1	1	2	4
<i>T</i> [K]	298(2)	218(2)	298(2)	298(2)
Measured reflections	16436	18256	14111	21099
Independent reflections	14420	9347	12251	15536
Final <i>R</i> ₁ , <i>wR</i> ₂ [<i>I</i> > 3 σ (<i>I</i>)]	0.0437	0.0316	0.0531	0.0617
9 , 10 ; <i>I</i> > 2 σ (<i>I</i>) 8]	0.1192	0.0736	0.1269	0.1514

absorption corrections were based on ψ scans of nine reflections, respectively ($\chi = 78$ to 102° , 360° scans in 10° steps in ψ).^[42] All structure determination calculations were carried out with SHELXTL NT 5.10 including SHELXS-97^[43] and SHELXL-97.^[44] Final refinements on F^2 were carried out with anisotropic thermal parameters for all non-hydrogen atoms in all cases. For **8**, the protons attached to the nitrogen atom of dppam and the cyclobutane ring were located and isotropically refined with fixed *U*. All other hydrogen atoms were included using a riding model with isotropic *U* values depending on the *U*_{eq} of the adjacent carbon atoms. The CH₂Cl₂ solvent molecules in **1**, **3**, **6**, **9**, **10** and **14** are disordered. Tables 1, 2 and 3 contain selected bond lengths and bond angles of all eight structures.

CCDC-628190 to -628197 contain the supplementary crystallographic data for this paper. These data can be obtained free of charge from The Cambridge Crystallographic Data Centre via www.ccdc.cam.ac.uk/datarequest/cif.

Acknowledgments

R. G., G. C. and A. D., and S. E., and M. F. thank the University of Innsbruck for post doctoral, PhD and diploma grants, respectively. This research was also financially supported by the Fonds zur Förderung der wissenschaftlichen Forschung, Vienna, Austria and the Tiroler Wissenschaftsfonds, Innsbruck, Austria. P. B. thanks Claudio Bianchini and Werner Oberhauser for helpful discussions.

- [1] C. Bianchini, H. M. Lee, A. Meli, W. Oberhauser, F. Vizza, P. Brüggeller, R. Haid, C. Langes, *Chem. Commun.* **2000**, 777–778.
- [2] C. Bianchini, G. Mantovani, A. Meli, W. Oberhauser, P. Brüggeller, T. Stampfl, *J. Chem. Soc., Dalton Trans.* **2001**, 690–698.
- [3] C. Bianchini, L. Gonsalvi, W. Oberhauser, D. Sémeril, P. Brüggeller, R. Gutmann, *Dalton Trans.* **2003**, 3869–3875.
- [4] Z. Freixa, P. W. N. M. van Leeuwen, *Dalton Trans.* **2003**, 1890–1901.
- [5] H. A. Mayer, W. C. Kaska, *Chem. Rev.* **1994**, *94*, 1239–1272.
- [6] W. Oberhauser, C. Bachmann, T. Stampfl, R. Haid, C. Langes, H. Kopacka, A. Rieder, P. Brüggeller, *Inorg. Chim. Acta* **1999**, *290*, 167–179.

- [7] R. Haid, R. Gutmann, T. Stampfl, C. Langes, G. Czermak, H. Kopacka, K.-H. Ongania, P. Brüggeller, *Inorg. Chem.* **2001**, *40*, 7099–7104.
- [8] R. Gutmann, G. Czermak, A. Dumfort, W. E. van der Veer, B. Hong, H. Kopacka, K.-H. Ongania, T. Bechtold, P. Brüggeller, *Inorg. Chem. Commun.* **2005**, *8*, 319–322.
- [9] I. O. Koshevoy, O. V. Sizova, S. P. Tunik, A. Lough, A. J. Poë, *Eur. J. Inorg. Chem.* **2005**, 4516–4520.
- [10] B. Cornils, W. A. Herrmann, R. Schlögl, C.-H. Wong, *Catalysis from A to Z*, Wiley-VCH, Weinheim, **2000**, pp. 279–282.
- [11] P. Maire, F. Breher, H. Schönberg, H. Grützmacher, *Organometallics* **2005**, *24*, 3207–3218.
- [12] a) J. J. Gambaro, W. H. Hohman, D. W. Meek, *Inorg. Chem.* **1989**, *28*, 4154–4159; b) R. R. Schrock, J. A. Osborn, *J. Am. Chem. Soc.* **1971**, *93*, 2397–2407.
- [13] R. Fornika, C. Six, H. Görls, M. Kessler, C. Krüger, W. Leitner, *Can. J. Chem.* **2001**, *79*, 642–648.
- [14] I. Schranz, G. R. Lief, S. J. Midstokke, L. Stahl, *Inorg. Chem.* **2002**, *41*, 6919–6927.
- [15] J. P. Cahill, A. P. Lightfoot, R. Goddard, J. Rust, P. J. Guiry, *Tetrahedron: Asymmetry* **1998**, *9*, 4307–4312.
- [16] F. Läng, F. Breher, D. Stein, H. Grützmacher, *Organometallics* **2005**, *24*, 2997–3007.
- [17] C. Laporte, C. Böhler, H. Schönberg, H. Grützmacher, *J. Organomet. Chem.* **2002**, *641*, 227–234.
- [18] Z. Duan, M. J. Hampden-Smith, E. N. Duesler, A. L. Rheingold, *Polyhedron* **1994**, *13*, 609–623.
- [19] L. Gonsalvi, H. Adams, G. J. Sunley, E. Ditzel, A. Haynes, *J. Am. Chem. Soc.* **2002**, *124*, 13597–13612.
- [20] a) W. Oberhauser, T. Stampfl, R. Haid, C. Langes, C. Bachmann, H. Kopacka, K.-H. Ongania, P. Brüggeller, *Polyhedron* **2001**, *20*, 727–740; b) W. Oberhauser, T. Stampfl, C. Bachmann, R. Haid, C. Langes, H. Kopacka, K.-H. Ongania, P. Brüggeller, *Polyhedron* **2000**, *19*, 913–923.
- [21] E. de Wolf, A. L. Spek, B. W. M. Kuipers, A. P. Philipse, J. D. Meeldijk, P. H. H. Bomans, P. M. Frederik, B.-J. Deelman, G. van Koten, *Tetrahedron* **2002**, *58*, 3911–3922.
- [22] C. Bianchini, P. Brüggeller, C. Claver, G. Czermak, A. Dumfort, A. Meli, W. Oberhauser, E. García Suárez, *Dalton Trans.* **2006**, 2964–2973.
- [23] M. J. Burk, J. E. Feaster, W. A. Nugent, R. L. Harlow, *J. Am. Chem. Soc.* **1993**, *115*, 10125–10138.
- [24] W. Oberhauser, C. Bachmann, T. Stampfl, R. Haid, C. Langes, A. Rieder, P. Brüggeller, *Polyhedron* **1998**, *17*, 3211–3220.
- [25] P. Nair, G. K. Anderson, N. P. Rath, *Organometallics* **2003**, *22*, 1494–1502.

- [26] H. Schumann, O. Stenzel, S. Dechert, F. Girgsdies, J. Blum, D. Gelman, R. L. Halterman, *Eur. J. Inorg. Chem.* **2002**, 211–219.
- [27] J. L. Bookham, D. M. Smithies, M. Thornton-Pett, *J. Chem. Soc., Dalton Trans.* **2000**, 975–980.
- [28] D. G. McCollum, G. P. A. Yap, A. L. Rheingold, B. Bosnich, *J. Am. Chem. Soc.* **1996**, *118*, 1365–1379.
- [29] D. Zhao, R. Bau, *Inorg. Chim. Acta* **1998**, *269*, 162–166.
- [30] A. Frick, V. Schulz, G. Huttner, *Eur. J. Inorg. Chem.* **2002**, 3129–3147.
- [31] A. Martín, A. G. Orpen, *J. Am. Chem. Soc.* **1996**, *118*, 1464–1470.
- [32] G. Liehr, G. Szucsányi, J. Ellermann, *J. Organomet. Chem.* **1984**, *265*, 95–106.
- [33] a) P. Bhattacharyya, R. N. Sheppard, A. M. Z. Slawin, D. J. Williams, J. D. Woollins, *J. Chem. Soc., Dalton Trans.* **1993**, 2393–2400; b) R. Haid, R. Gutmann, G. Czermak, C. Langes, W. Oberhauser, H. Kopacka, K.-H. Ongania, P. Brüggeller, *Inorg. Chem. Commun.* **2003**, *6*, 61–67.
- [34] a) T. Stampfl, G. Czermak, R. Gutmann, C. Langes, H. Kopacka, K.-H. Ongania, P. Brüggeller, *Inorg. Chem. Commun.* **2002**, *5*, 490–495; b) T. Stampfl, R. Haid, C. Langes, W. Oberhauser, C. Bachmann, H. Kopacka, K.-H. Ongania, P. Brüggeller, *Inorg. Chem. Commun.* **2000**, *3*, 387–392.
- [35] V. Schulz, A. Frick, G. Huttner, *Eur. J. Inorg. Chem.* **2002**, 3111–3128.
- [36] C. Bianchini, W. Oberhauser, A. Orlandini, C. Giannelli, P. Frediani, *Organometallics* **2005**, *24*, 3692–3702.
- [37] C. P. Casey, S. C. Martins, M. A. Fagan, *J. Am. Chem. Soc.* **2004**, *126*, 5585–5592.
- [38] Preliminary catalytic hydroformylation experiments of 1-hexene to yield the corresponding linear and branched aldehydes by using [Rh₂(η⁴-cod)₂(dppcb)](PF₆)₂ (**1**) as a precatalyst exhibited good activity and moderate regioselectivity in *n*-heptanal.
- [39] N.-W. Tseng, J. Mancuso, M. Lautens, *J. Am. Chem. Soc.* **2006**, *128*, 5338–5339.
- [40] Z. Otwinowski, W. Minor in *Methods in Enzymology Vol. 276: Macromolecular Crystallography, Part A* (C. W. Carter Jr, R. M. Sweet, Eds.), Academic Press, New York, **1997**, pp. 307–326.
- [41] *SHELXTL*, version 4.2, Siemens Analytical X-ray Instruments, Madison, WI, **1991**.
- [42] A. C. T. North, D. C. Phillips, F. S. Mathews, *Acta Crystallogr., Sect. A* **1968**, *24*, 351–359.
- [43] G. M. Sheldrick, *Acta Crystallogr., Sect. A* **1990**, *46*, 467–473.
- [44] G. M. Sheldrick, *SHELXL-97: Program for Refinement of Crystal Structures*, University of Göttingen, Germany, **1997**.

Received: December 19, 2006
Published Online: May 23, 2007